JOURNAL OF MATERIALS SCIENCE 33 (1998) 4843–4855

X-ray photoelectron spectroscopic investigation of the durability of siloxane plasma polymer coatings in a steam atmosphere

M. P. BONNAR, J. I. B. WILSON*, B. M. BURNSIDE, R. L. REUBEN
*Department of Mechanical and Chemical Engineering, and *Department of Physics, Heriot-Watt University, Riccarton, Edinburgh EH14 4AS, UK*
E-mail: j.i.b.wilson@hw.ac.uk

T. R. GENGENBACH, H. J. GRIESSER
CSIRO Division of Chemicals and Polymers, Clayton, Victoria 3169, Australia

GRAHAM BEAMSON
RUSTI, Daresbury Laboratory, Daresbury, Warrington, Cheshire WA4 4AD, UK

Thin-film plasma polymer coatings were deposited on to titanium, stainless steel and 70/30 copper-nickel substrates from hexamethyldisiloxane (HMDSO) as potential permanent promoters of dropwise condensation of steam. Long-term durability condensation tests showed that HMDSO films on titanium exposed to low-velocity steam performed well with some lifetimes in excess of 12 000 h. X-ray photoelectron spectroscopy (XPS) was used to monitor the dependence of chemical composition of the films on the deposition conditions and it was shown that composition was not critically dependent on deposition conditions. Additionally, XPS was used to monitor chemical composition before and after exposure of specimens to steam in an attempt to identify the failure mechanisms for films which had ceased to sustain dropwise condensation over their entire surface. Furthermore, short tube sections were coated with plasma-polymerized HMDSO and exposed to steam at elevated velocities. In this case the durability was poor and this is attributed to water droplet impingement erosion on the tube surfaces. This was confirmed by a subsequent test where no water droplets were present in the steam flow and the coating lifetime was seen to increase.

1. Introduction

Thin-film coatings deposited by low-pressure plasma chemical vapour deposition (CVD) have received considerable attention since it was realised that thin, durable, pinhole-free polymer films could be deposited from a variety of organic precursors which do not readily polymerize by traditional methods [1–4]. Particular interest has focused on organosilicon precursors because of the high deposition rates which can be attained with these monomers. The plasma deposition technique gives control over chemical and structural composition of the film and hence its properties, by varying the deposition conditions [5].

Hexamethyldisiloxane (HMDSO), the organosilicon precursor used to form films in this study, is one of the most popular monomers for plasma polymerization and has been used by many workers, as summarized in review articles [6, 7]. Its plasma polymers have been investigated for various intended uses and have found application in the production of scratch-resistant coatings for ophthalmic lenses [8] as well as corrosion-resistant layers for the automotive industry [9]. Whilst most previous studies refer to plasma deposition with radio frequency (r.f., 13.56 MHz) or microwave (MW, 2.45 GHz) power sources, d.c. plasma polymerization has also been reported [10], including a variant in which gold from the cathode was sputtered into the plasma polymer layer [11]. It is usual to heat the substrate when depositing films by plasma CVD, but cold substrates have been used in experiments to deposit silicon oxide from HMDSO/O_2 [12] or HMDSO/evaporated-SiO [13] and in deposition of polymers from various siloxane precursors [14]. The production of silicon oxide from HMDSO is a common objective of many researchers, who usually reduce the carbon content by adding oxygen rather than by applying such a high substrate temperature that the deposition rate is reduced or the substrate damaged [12, 15, 16]. The optical properties of plasma-polymerized HMDSO have been reported by many, extending from UV to IR regions of the spectrum (e.g. [17–19]), with extensive use of Fourier transform–infrared spectroscopy (FT–IR) to elucidate the hydrogen bonding as a function of the deposition conditions (e.g. [12, 13, 15, 17, 19–21]).

Methyl abstraction from the monomer molecule is thought to be the dominant reaction step in the plasma

polymerization of HMDSO, as the coatings are found by XPS to be depleted in carbon and show a silicon peak structure and binding energy position indicative of various oxidation states [22]. In other words, a considerable fraction of the silicon atoms in the HMDSO plasma polymer possess more than one oxygen-atom neighbour. Other studies have investigated the effect of adding molecular oxygen to the plasma atmosphere during polymerization of HMDSO [23, 24] and it is now understood that the addition of even small amounts of molecular oxygen can enhance methyl abstraction, hence producing a predominantly "silica-like" deposit.

The present work is part of an investigation of HMDSO plasma polymers as durable coatings on metal substrates, for the promotion of dropwise condensation (DWC) of steam on utility turbine condenser tubes. A detailed account of the motivation and plasma polymerization process has been reported previously [25]. This intended application requires a hydrophobic coating. Accordingly, the production of a largely silica-like oxidized film was undesirable; we needed to define conditions for the fabrication of a coating which retains to a sufficient extent an organic structure. Therefore, the HMDSO precursor has been used undiluted by any other gas which might result in increased methyl fragmentation. In the present work, the influence of deposition parameters on composition and structure of HMDSO plasma coatings on titanium substrates was investigated by XPS, followed by a study of the long-term durability of specimens exposed to steam. We have also analysed reasons for failure to sustain DWC, using XPS to monitor chemical and structural changes before and after exposure to steam. XPS elemental mapping has also been used to study areas of failed test specimens where the coating appeared to have been removed.

2. Experimental procedure

Based on observations of a number of hydrophobic plasma polymers, we have selected coatings deposited from HMDSO which were most consistently reliable during long-term testing. These coatings were deposited on to titanium, stainless steel and 70/30 copper-nickel substrates. Coated titanium specimens (25 mm × 15 mm × 1 mm) have been found to be the most promising for the intended DWC application; to date, our best coatings have survived long-term testing for 12 000 h continuous steam exposure. The films were deposited using a parallel plate r.f. plasma system described previously [26] and shown schematically in Fig. 1. The deposition conditions (r.f. power, monomer flow rate, pressure, substrate temperature) were optimized by a statistically designed set of experiments (see selected values in Table I). Coating thickness, measured using a Dektak 3030 surface profilometer, was between 200 and 500 nm. Water-droplet contact-angle measurements were made on a representative specimen from each of the set of 16 deposition experiments, before exposure to dry steam at atmospheric pressure, and 100 °C, in a long-term condensation test cell. Advancing contact angles for deposited films were found to be in the range 95°–105°. In each of the 16 deposition experiments, two of each substrate material were coated, one of which went into the long-term durability test while the other was kept for XPS analysis. Hence a sample from each set of experimental conditions on each of the three substrate materials was analysed by XPS. In addition, representative samples which had been exposed to steam for a period of 5000 h, some of which had failed to sustain DWC, were removed from the long-term steam test for XPS analysis.

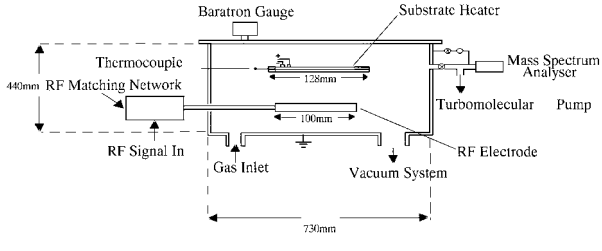

Figure 1 Schematic diagram of the r.f. plasma deposition system.

TABLE I Deposition conditions for the HMDSO films

Sample	RF power (W)	Pressure (torr[a])	Temp. (°C)	Flow
1164	25	0.08	100	10
1165	75	0.12	100	20
1166	25	0.1	150	20
1167	100	0.08	250	20
1168	75	0.14	150	10
1169	50	0.08	150	30
1170	100	0.1	200	10
1171	50	0.14	200	20
1172	100	0.14	100	30
1174	25	0.12	200	30
1175	50	0.12	250	10
1176	75	0.1	250	30
1177	50	0.1	100	40
1178	25	0.14	250	40
1179	100	0.12	150	40
1180	75	0.08	200	40

[a]1 torr = 133.322 Pa.

Furthermore, titanium tube sections, 19 mm diameter, 110 mm long, with a wall thickness of 0.5 mm, were coated with the HMDSO plasma polymer under those conditions which produced the most durable and hydrophobic films according to long-term testing of coated flat samples. Coated tubes were required for measurements of overall heat-transfer coefficient [27]. The apparatus used to coat the tube geometry was constructed in-house and consisted of a cylindrical electrode with the substrate tube mounted on a concentric rod heater. The discharge was confined to the inside of the cylindrical electrode and r.f. power density was scaled to match that used for the flat specimens. Details of tube-coating conditions and results from heat-transfer tests will be presented in a subsequent publication. Coated tubes also underwent XPS analysis after being exposed to steam at elevated velocities; these results are presented in Section 4.3.

3. XPS analysis

Samples were not exposed to any form of precleaning before XPS analysis. A brief ion-bombardment is often used to remove the top nanometer or so of the material and hence any adventitious carbon contamination

[28]. Such pre-treatment may, however, alter the surface composition and structure, particularly in the case of plasma polymers.

XPS analysis of the specimens was carried out using two different instruments: firstly, a Scienta ESCA300 spectrometer at CCLRC Daresbury Laboratory, UK, and secondly a Kratos AXIS HSi spectrometer at the Division of Chemicals and Polymers, CSIRO, Australia. The results are complementary because the first set of analyses were performed with samples mounted on conducting double-sided tape, and the second set with electrically isolated samples. Consequently, we have been able to discriminate between functionalities formed on the coating surface and adventitious carbon in intimate contact with the titanium substrate.

3.1. Scienta ESCA300 spectrometer

The monochromatized AlK (1486.7 eV) X-ray source of the ESCA300 spectrometer was operated at 2.8 kW (14 kV, 200 mA). Survey scans were recorded at 150 eV pass energy, 1.9 mm slit width, giving an overall instrument resolution of 0.53 eV [29, 30]. Region spectra were recorded at 150 eV pass energy, 0.5 mm slit width, giving an instrument resolution of 0.35 eV [29, 30]. Charge compensation was achieved using a Scienta flood gun set to 2 eV kinetic energy. (Owing to the ejection of photoelectrons from the surface of a sample undergoing XPS examination, areas of the sample which are insulating will become positively charged, resulting in a shift to higher energy of the XPS spectra. If a charge compensation electron flood gun is used, as in the present work, the sample usually acquires a negative charge, resulting in a shift of the entire spectrum of insulating areas of the sample to low binding energy. This shift can be several electron volts, depending on the type and level of charge compensation which is used. This charge shift is traditionally corrected by referencing one of the component peaks to the binding energy of a known element in the sample; however, this can become complex in the case of differential charging between the substrate and the coating.)

The samples were mounted on standard stainless steel stubs and introduced to the spectrometer via a fast-entry air lock and preparation chamber. The pressure in the analysis chamber during XPS analysis was $\sim 10^{-8}$ mbar (1 Pa $= 10^{-2}$ mbar). Samples were analysed at electron take-off angles of 10°, 45° and 90° (relative to the sample surface). Spectra were quantified using a straight-line baseline under the core-line envelopes and using C 1s, O 1s, Si 2p and Na 1s sensitivity factor measures from compounds of known stoichiometry. For Ti 2p, the sensitivity factor provided by the instrument manufacturer was used.

3.2. Kratos AXIS HSi spectrometer

For standard XPS analyses, the monochromatized Al*K* source was operated at a power of 300 W (15 kV × 20 mA), with the hemispherical analyser in the fixed analyser transmission mode and the standard aperture (1 mm × 0.5 mm). The total pressure in the main vacuum chamber during analysis was of the order of 10^{-8} mbar.

All elements present were identified from survey spectra acquired at 320 eV pass energy. For further analysis, high-resolution spectra were recorded from individual peaks at 20 eV pass energy (resolution better than 0.45 eV). The atomic concentrations of all elements were calculated with integral peak intensities (using a non-linear Shirley-type background) and the sensitivity factors supplied by the manufacturer.

Each specimen was analysed at an electron take-off-angle of 90° (relative to the sample surface). Assuming a value of approximately 2–3 nm for the electron attenuation length of a C 1s photoelectron in a polymeric matrix, this translates into an approximate value for the XPS analysis depth (from which 95% of the detected signal originates) of 5–10 nm.

Charge neutralization in the AXIS HSi spectrometer employs the magnetic immersion lens which is used as part of the imaging system. A bias electrode directs low kinetic energy electrons (1–4 eV) generated by a heated tungsten filament into the magnetic field of the immersion lens which, in turn, transports the electrons to the sample. This leads to a very uniform and consistent neutralization of charge build-up during analysis [31].

For this investigation, use was also made of the mapping capabilities of the AXIS HSi spectrometer: the spatial distribution of any element may be mapped across the sample surface by monitoring the intensity of the corresponding photoelectron signal as the analysis spot is rastered over a preselected area. In this case, the non-monochromatized X-ray source is used (either Al*K* or Mg*K* radiation) to ensure a uniform X-ray flux across the surface to be analysed. The mapped area usually measures (1.2 × 1.2) mm^2 and the spatial resolution (analysis area) can be selected by using different apertures (120, 60 or 30 mμ. In this study, the 120 μm aperture was selected due to time constraints; reducing the aperture size leads to a substantial loss of signal intensity and hence data acquisition times have to be increased in order to obtain data with acceptable signal/noise ratios. Intensity variations across the surface due to spatial non-uniformity of the X-ray flux or due to topographic effects are corrected for by simultaneously acquiring two maps of the same area: one, using the peak maximum of the actual photoelectron signal, and a second one using the background signal at a binding energy several electron-volts below the peak (background map). The difference of these two maps displays only the signal variations due to variations of the peak height. This assumes that charge compensation is uniform across the mapped area, thus leading to a constant shift of the energy scale.

Furthermore, multipoint analysis with small area sampling allows the operator to select from a map individual points of interest for a full spectroscopic analysis at the same spatial resolution ("spatially keyed spectroscopy"). In addition to giving the same spectroscopic information as a standard XPS analysis, this facility allows the operator to verify the above-mentioned assumption regarding spatially uniform charge compensation.

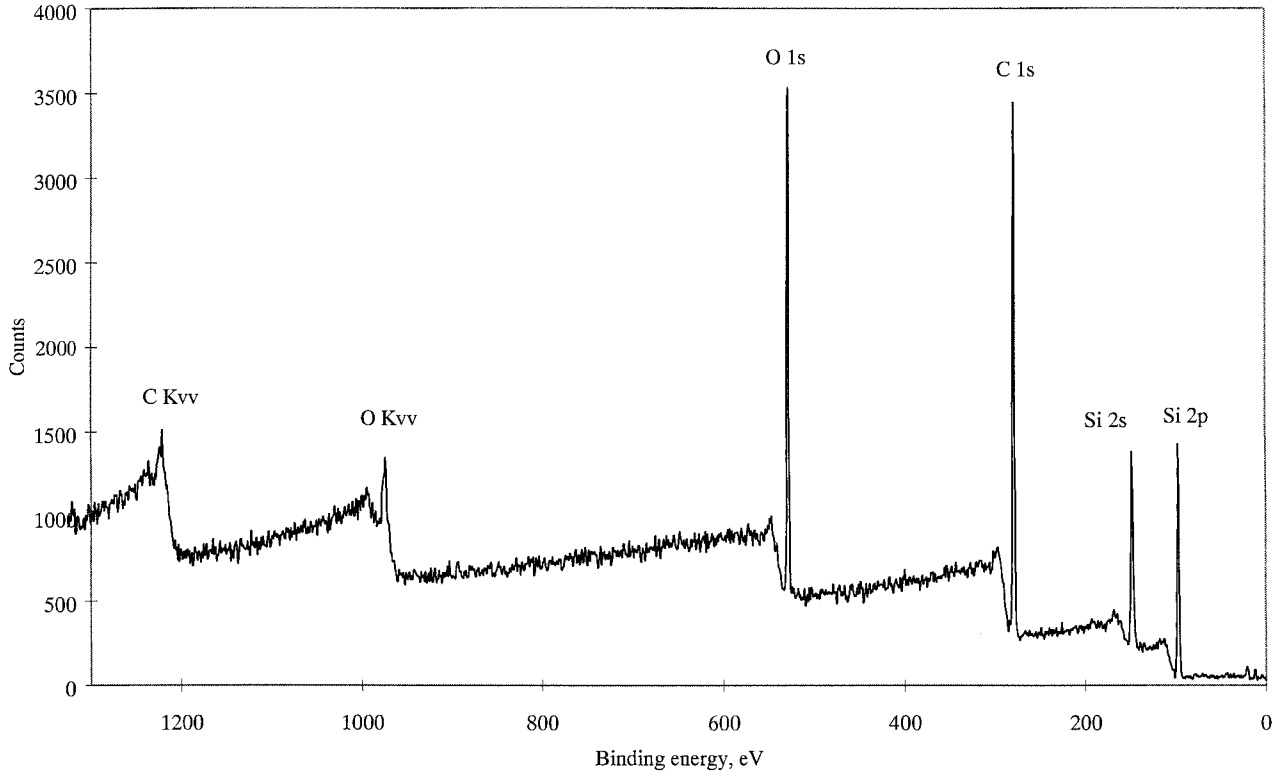

Figure 2 XPS survey scan of a typical HMDSO plasma polymer film on a titanium substrate – as deposited (electron take-off-angle = 10°).

4. Results

4.1. As-deposited plasma polymer coatings

As-deposited plasma-polymerized HMDSO coatings on titanium substrates were examined using the ESCA300 spectrometer. XPS survey scans of all the samples showed only the presence of C, O and Si; see Fig. 2. Fig. 3 shows typical C 1s, O 1s and Si 2p spectra. Quantification of the spectra recorded at 10° take-off-angle (relative to the sample surface) gave similar elemental compositions for all samples, regardless of

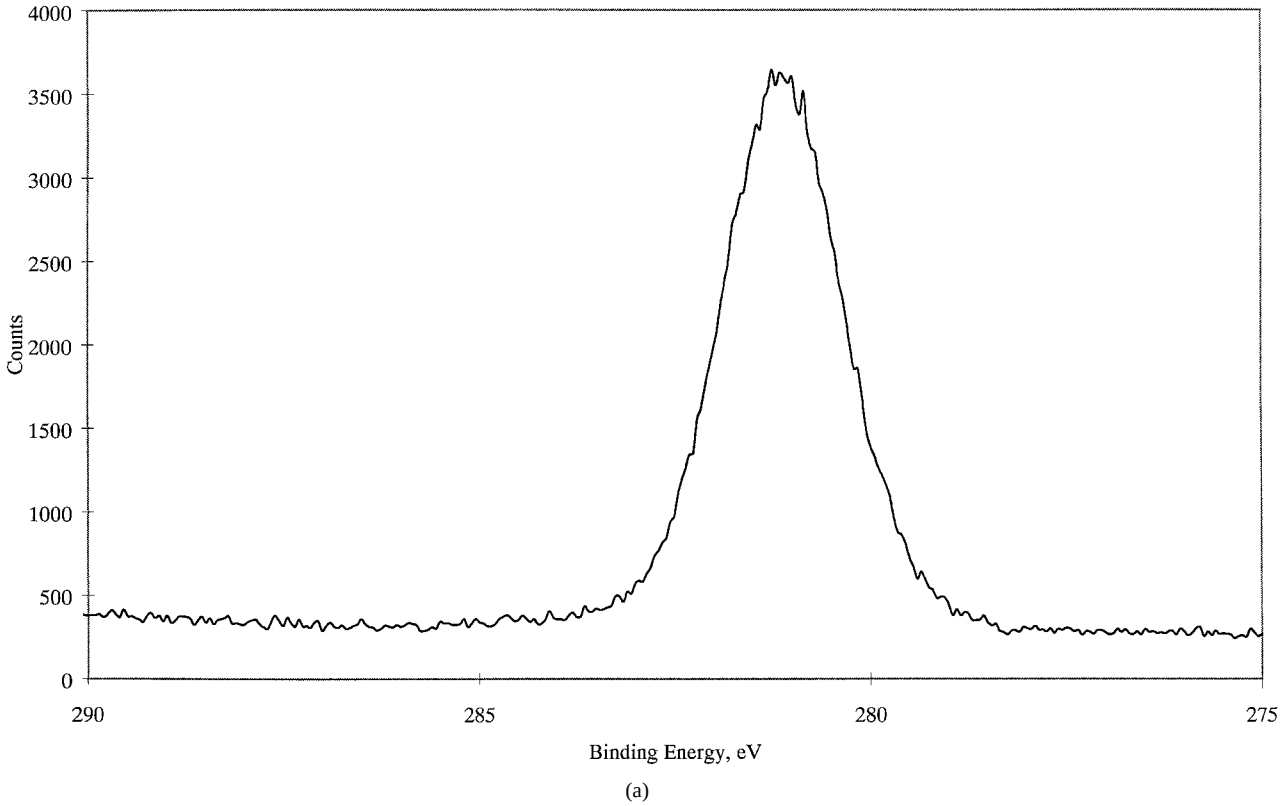

(a)

Figure 3 Typical photoelectron spectra of as-deposited HMDSO plasma polymer, Scienta ESCA300 spectrometer (electron take-off-angle = 10°) (a) Carbon 1s spectrum. (b) Oxygen 1s spectrum. (c) Silicon 2p spectrum. (continued)

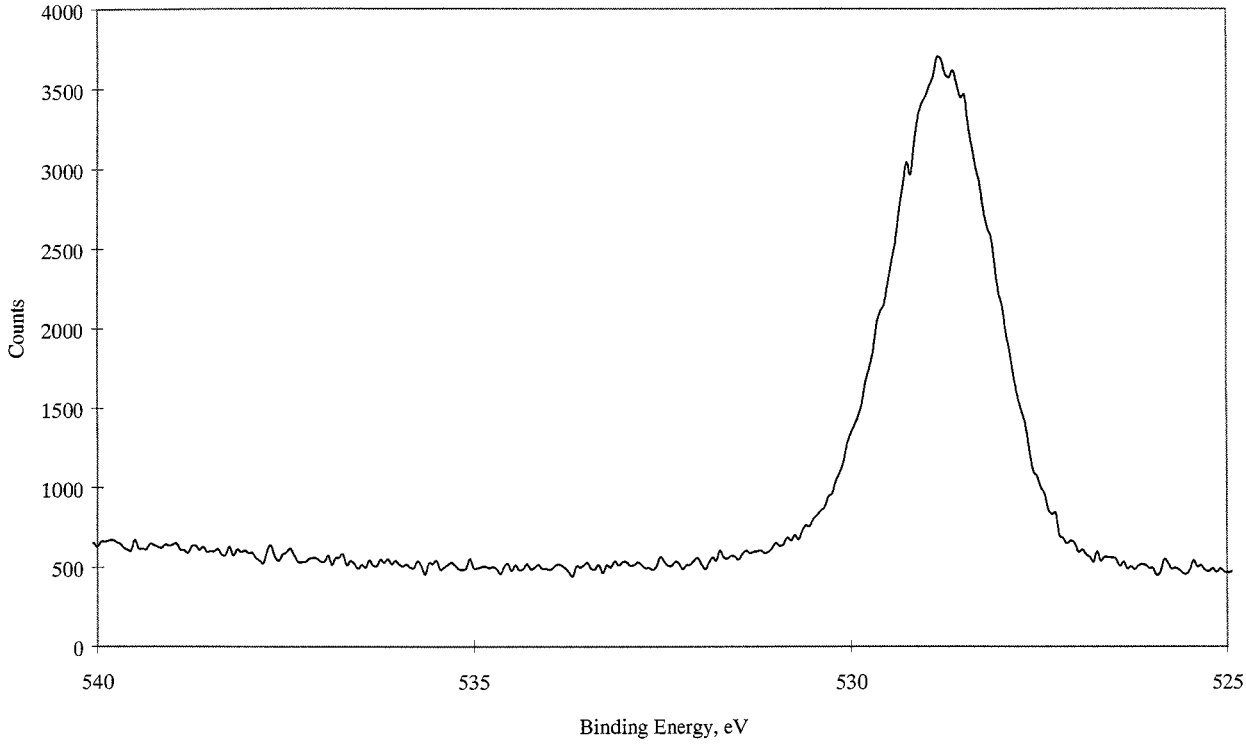

(b)

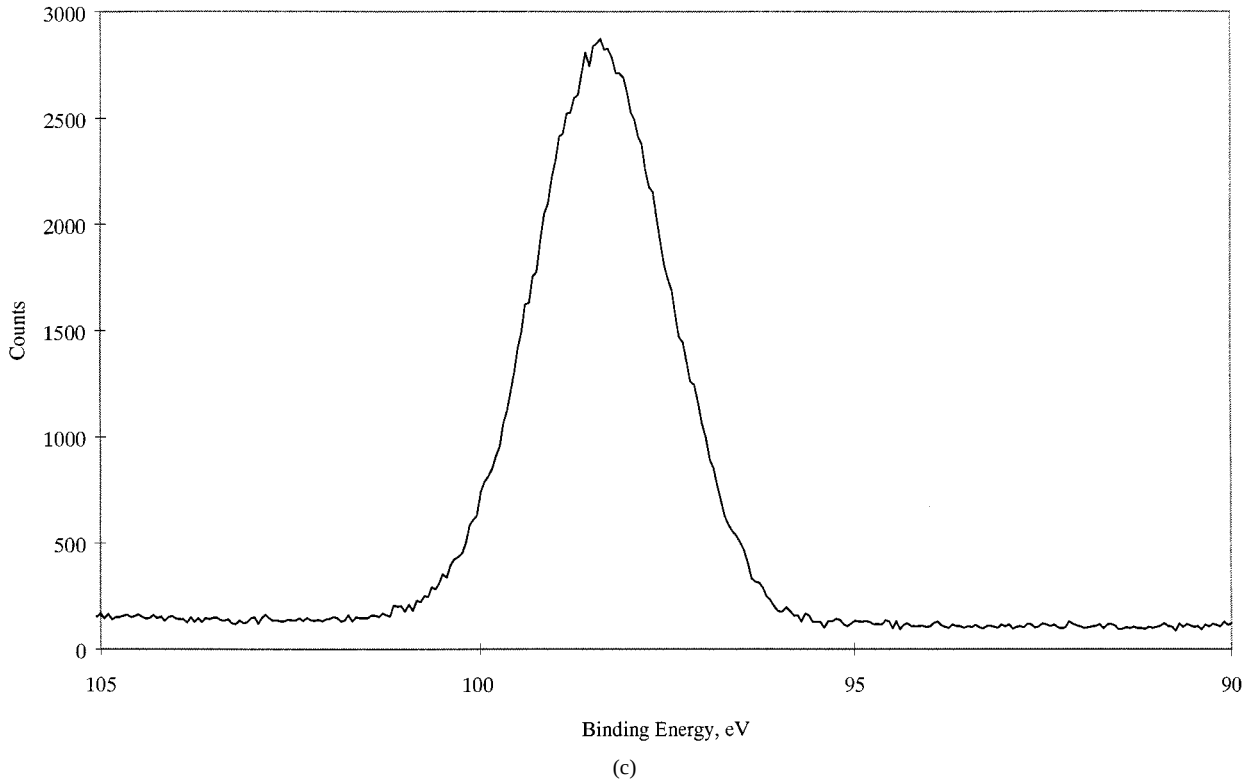

(c)

Figure 3 (continued).

the plasma deposition conditions, i.e. ~ 55 at % C, 17 at % O and 27 at % Si (HMDSO composition = 67 at % C, 11 at % O, 22 at % Si) neglecting hydrogen content; see Table II. Fig. 4 shows plots of film composition versus the plasma process variables: r.f. power, substrate temperature and monomer dwell time ((pressure × volume)/flow rate), and reveals only small changes in composition with deposition conditions. This is in agreement with a study carried out by Sacher *et al.* [32]. Several experiments were performed at higher take-off-angles (45° and 90°) and although the increase in sampling depth is slight, small increases in oxygen were detected when compared with scans for the same samples at the original 10° take-off-angle. This result is consistent with either a layer of hydrocarbon surface contamination or, more likely, methyl and trimethysilyl terminating functionalities on a –Si–O–Si– polymer backbone as reported previously [22].

C 1s spectra of as-deposited films recorded with the ESCA300 spectrometer generally showed a single component with a measured binding energy of ∼281 eV. We assign this to the C–Si environment with a charge-corrected binding energy of 284.4 eV [30]. This gives corrected O 1s and Si 2p binding energies of 531.8 and 101.6 eV, close to the literature values (532.0 and 101.8, respectively [30]) for polydimethylsiloxane.

Data obtained using the Kratos AXIS HSi spectrometer showed the as-deposited HMDSO films on titanium to have a composition of 47 at % C, 23 at % O and 27 at % Si. The take-off-angle was 90° relative to the sample surface. This agrees with the higher oxygen content observed at greater take-off angles on the Scienta system, with the silicon content remaining constant. The C 1s, O 1s and Si 2p region spectra showed

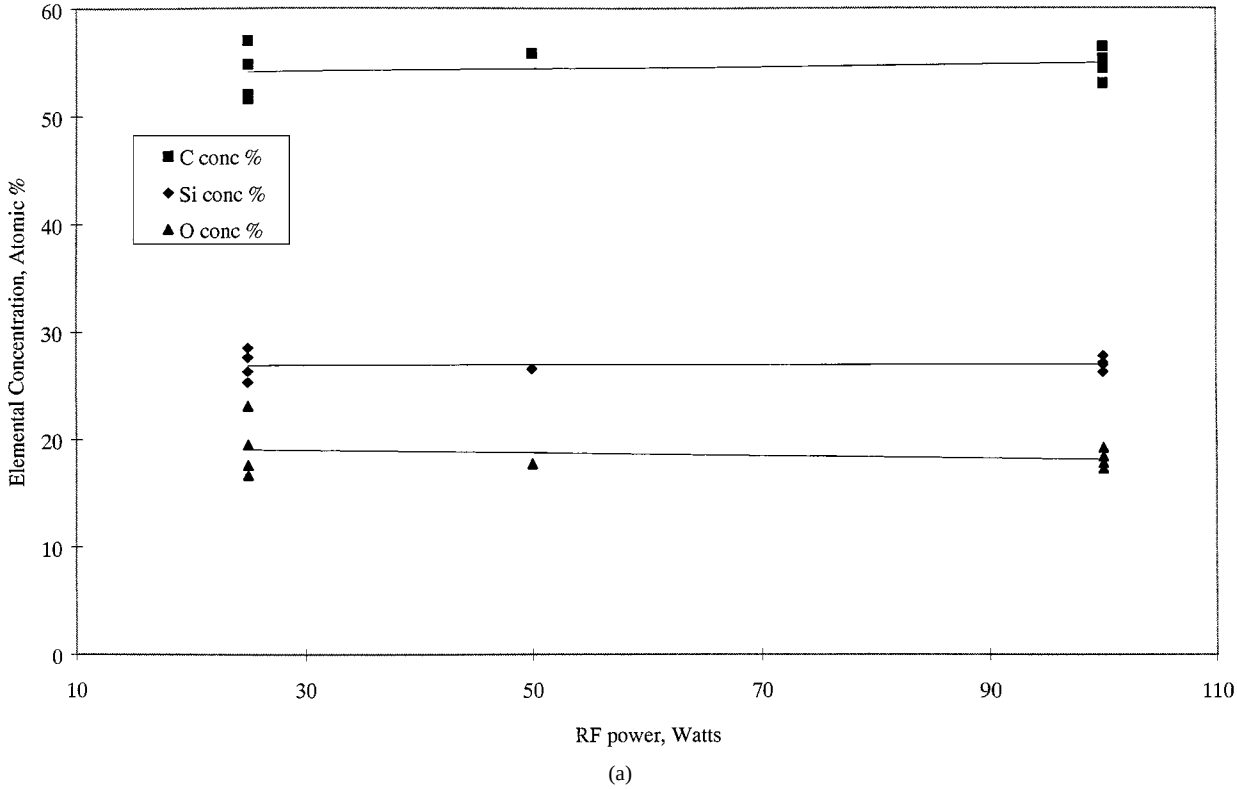

(a)

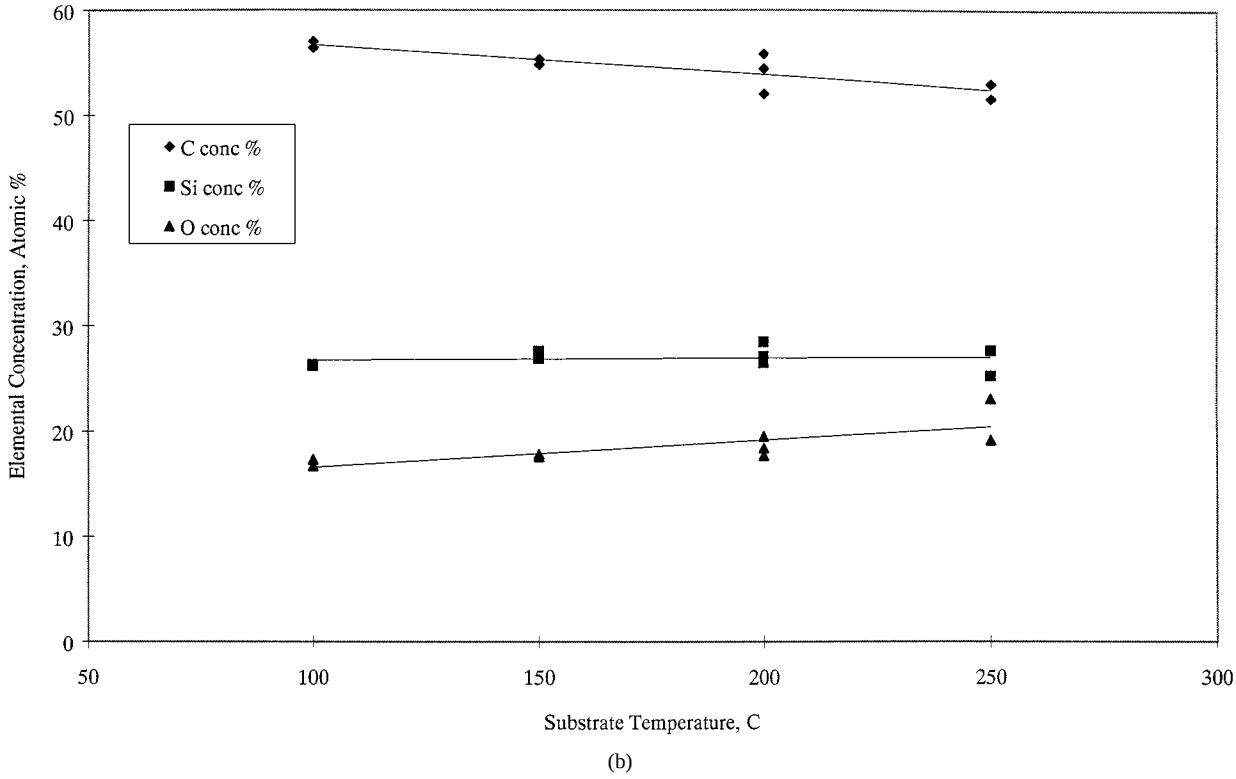

(b)

Figure 4 Elemental surface composition as determined by XPS versus three different plasma deposition parameters for plasma-polymerized HMDSO film as-deposited. (a) R.f. power. (b) Substrate temperature. (c) Dwell time. (■) C, (♦) Si, (▲) O. (continued).

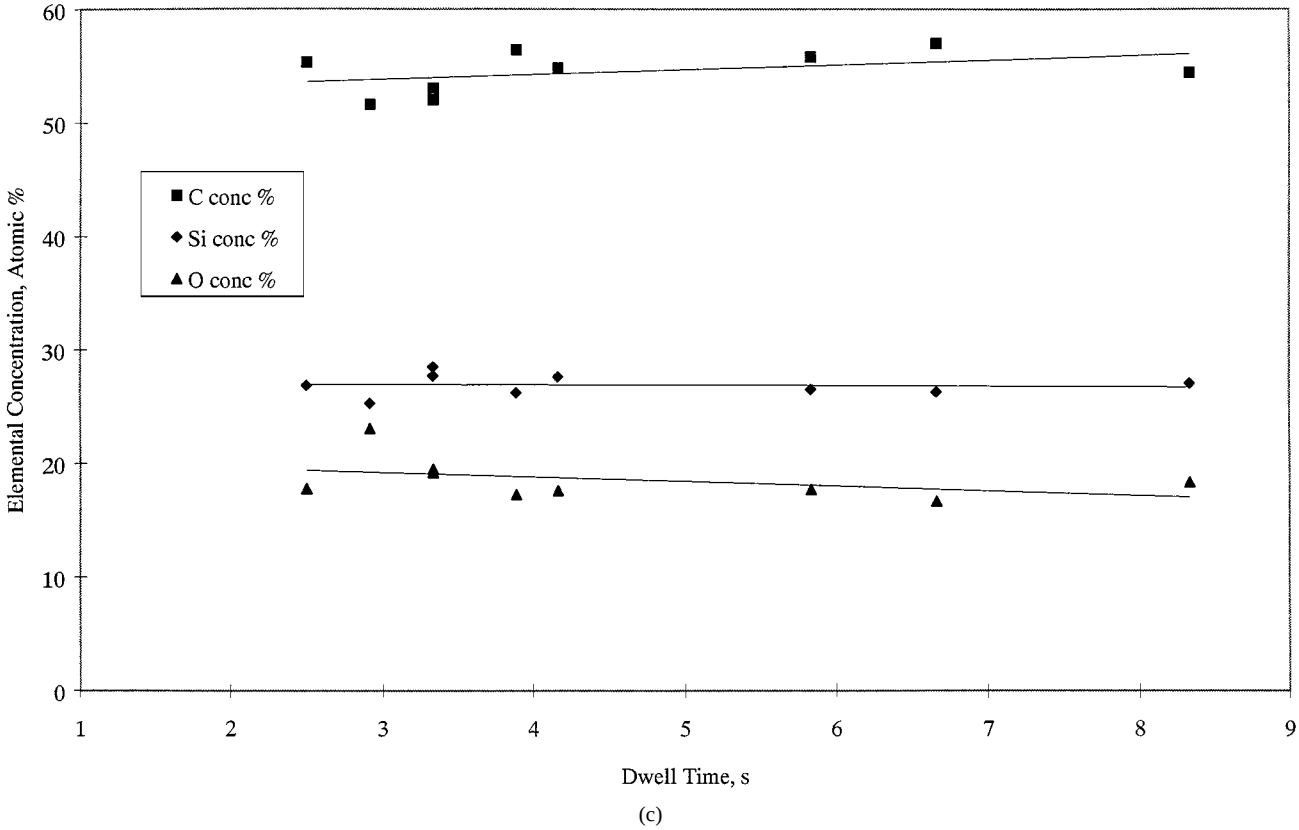

(c)

Figure 4 (continued).

TABLE II Elemental atomic concentrations for plasma-polymerized HMDSO on titanium, including XPS sensitivity factors, but neglecting any hydrogen content

Sample	Steam test pass/fail	Concentration (at %) C	O	Si	Ti
1164 - T2	–[a]	57.0	16.7	26.3	0
1166 - U2	–	54.8	17.6	27.6	0
1167 - S2	–	53.0	19.2	27.7	0
1170 - R2	–	54.4	18.4	27.1	0
1171 - C2	–	55.8	17.7	26.5	0
1172 - Q4	–	56.4	17.3	26.2	0
1174 - V2	–	52.0	19.5	28.5	0
1178 - W2	–	51.6	23.1	25.3	0
1179 - F2	–	55.3	17.8	26.9	0
1171 - D2	Passed	36.7	39.4	12.2	11.7
1179 - E2	Failed	30.5	45.4	7.8	16.4

[a]"–", No steam test.

charge-corrected binding energies of ∼ 284.4, 532.0, and 101.7 eV (again assigning the dominant C 1s component to C–Si at 284.4 eV), close to binding energies obtained with the ESCA300 spectrometer.

4.2. Steam-tested films

4.2.1. Standard XPS

After exposure of the coated titanium substrates to steam for ∼ 5000 h, XPS survey scans showed signals due to the substrate, indicating delamination or thinning of the polymer; see Fig. 5. A stronger substrate signal was detected from coatings which had failed to maintain dropwise condensation. Relative to the as-deposited coatings, steam-treated coatings showed a reduction in the concentration of silicon and carbon and an increase in oxygen and titanium; see Table II.

C 1s spectra of steam-treated samples recorded on the ESCA300 spectrometer (samples mounted with conducting double-sided tape) showed a low binding energy component at ∼ 281 eV and a higher one at ∼ 285 eV, see Fig. 6a. Referencing the low-binding energy component to 284.4 eV brings the higher one close to 289 eV, suggesting CO_2R/CO_2H functionalities [30]. However, the C 1s spectra of similar samples recorded in the Kratos AXIS HSi spectrometer (samples mounted with insulating double sided-tape) showed the high binding energy component as being of very low intensity; see Fig. 6b. Our conclusion is that there is, in fact, very little CO_2R/CO_2H functionality present at the surface of the steam-treated polymer samples and that in the ESCA300 spectra the component detected at a measured binding energy of ∼ 285 eV is due to either plasma polymer or adventitious hydrocarbon contamination in intimate contact with the titanium substrate. Such material would be expected at a measured binding energy of ∼ 285 eV. Hence the use of conducting double-sided tape to mount the samples generated differential charging between the substrate and thick plasma polymer overlayer, allowing detection of a very thin layer of either polymer or hydrocarbon contamination left on the substrate after steam testing.

The ESCA300 spectra show that the level of adventitious carbon or intimate polymer present on the surface increased with exposure time to steam and it is thought that this is due to more of the substrate being uncovered as the testing proceeds, resulting in more of the adventitious carbon/polymer present at the interface being exposed.

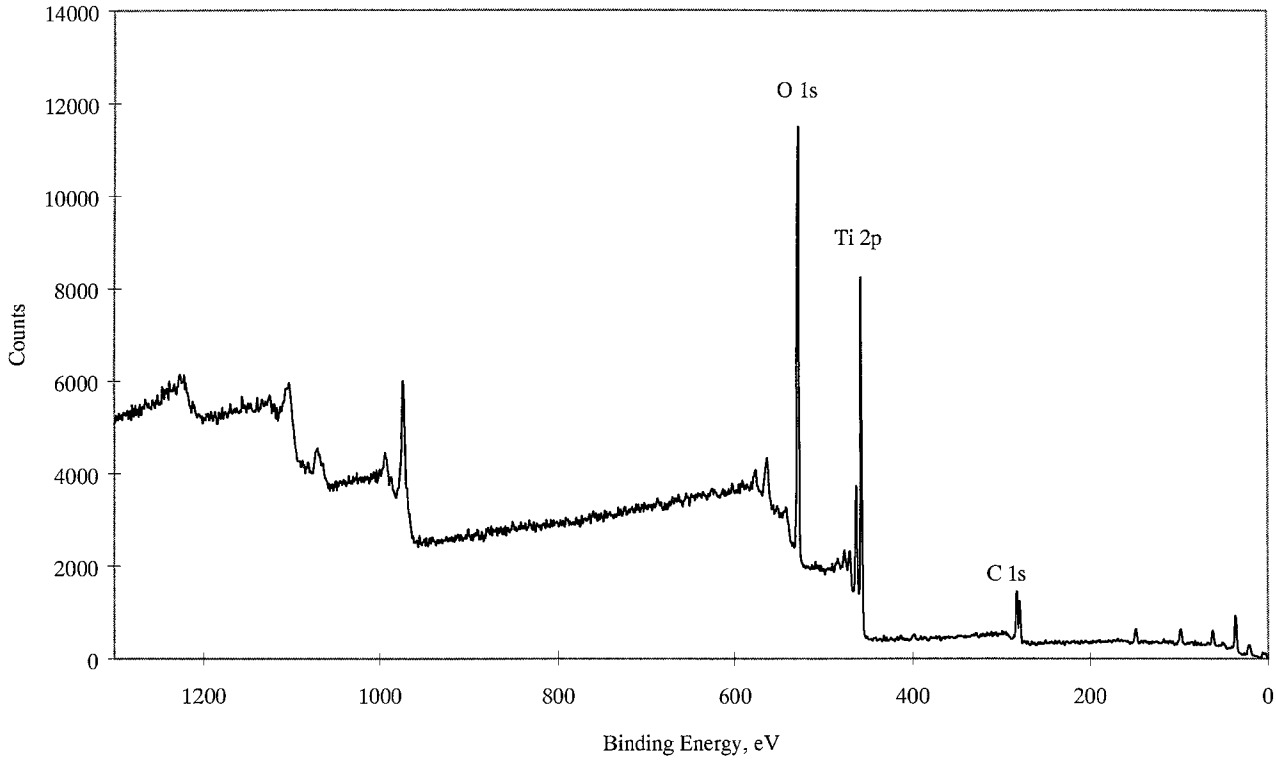

Figure 5 Typical XPS survey scan of a specimen which had failed to sustain dropwise condensation after ~5000 steam exposure, ESCA300 spectrometer (electron take-off-angle = 10°).

Many of the flat titanium test specimens which had undergone long-term steam testing and failed, exhibited a failure mechanism where islands of the coating had been removed. The size of these islands varied, but in general were several square millimetres in area. The reason for this localized detachment is unclear at this stage but initial scanning electron microscope and energy-dispersive X-ray (EDX) images have shown the presence of Al_2O_3 filled "pits" in the surface of the titanium substrate after film failure. An electron micrograph of an area of the substrate after coating failure can be seen in Fig. 7. The dark areas on the surface were identified as Al_2O_2 by EDX analysis. Although the presence of this contamination was surprising, an obvious source would be the sample polishing procedure prior to coating which consisted of a rough lap with an Al_2O_3 abrasive followed by a fine polish with 6 μm diamond paste. It is thought that pits may be the remains of original surface topography which have not been completely polished out. During lapping, these pits have trapped Al_2O_3 which may have hardened on drying, making it very difficult to remove. Diamond paste may also have been trapped in these pits which would account for the high levels of carbon detected at the coating/substrate interface.

Previous work by Griesser identified corrosion-induced pinholes in HMDSO plasma polymer coatings deposited on Co_4Ni films [33]. In the present case, it is thought that moisture may have permeated the coating to the metal substrate, resulting in either corrosive attack at the interface, or hydrolysis and subsequent expansion of the Al_2O_3, both resulting in localized film failure. Coating delamination did not occur with either of the other substrate materials (CuNi or 304 Stainless) nor on failed tube surfaces: because no Al_2O_3 contamination was detected, this suggests a different failure mechanism, such as a greater susceptibility to interfacial oxidation.

4.2.2. XPS mapping

The Kratos AXIS HSI system was used to perform XPS area mapping on HMDSO plasma coatings on titanium samples which had failed long-term steam tests, in an attempt to study in more detail the failure mechanism and the nature of the substrate/coating interface. Fig. 8 displays two maps; one (a) was recorded using the Ti $2p_{3/2}$ signal (representing the substrate material), the other map (b) was acquired using the Si 2p signal (representing the coating material). Clearly, the maps are complementary: across most of the mapped area, the HMDSO plasma coating had been largely removed during steam testing as indicated by the low Si 2p intensity and high Ti $2p_{3/2}$ intensity. In the lower left-hand corner of the map, however, a coating of considerable thickness was still detectable (high Si 2p intensity, low Ti $2p_{3/2}$ intensity).

For further spectroscopic analysis, four points were selected on these maps as indicated in Fig. 8: point 1 was located within an area of high Ti $2p_{3/2}$ intensity, point 2 in the lower left-hand corner (highest Si 2p intensity), and points 3 and 4 were located in intermediate areas (medium substrate signal intensity and low coating signal intensity). Fig. 9 shows the O 1s and Si 2p photoelectron spectra acquired at points 1, 2 and 3 on the sample (spectra for point 4 are not shown because data from points 3 and 4 were very similar). The low

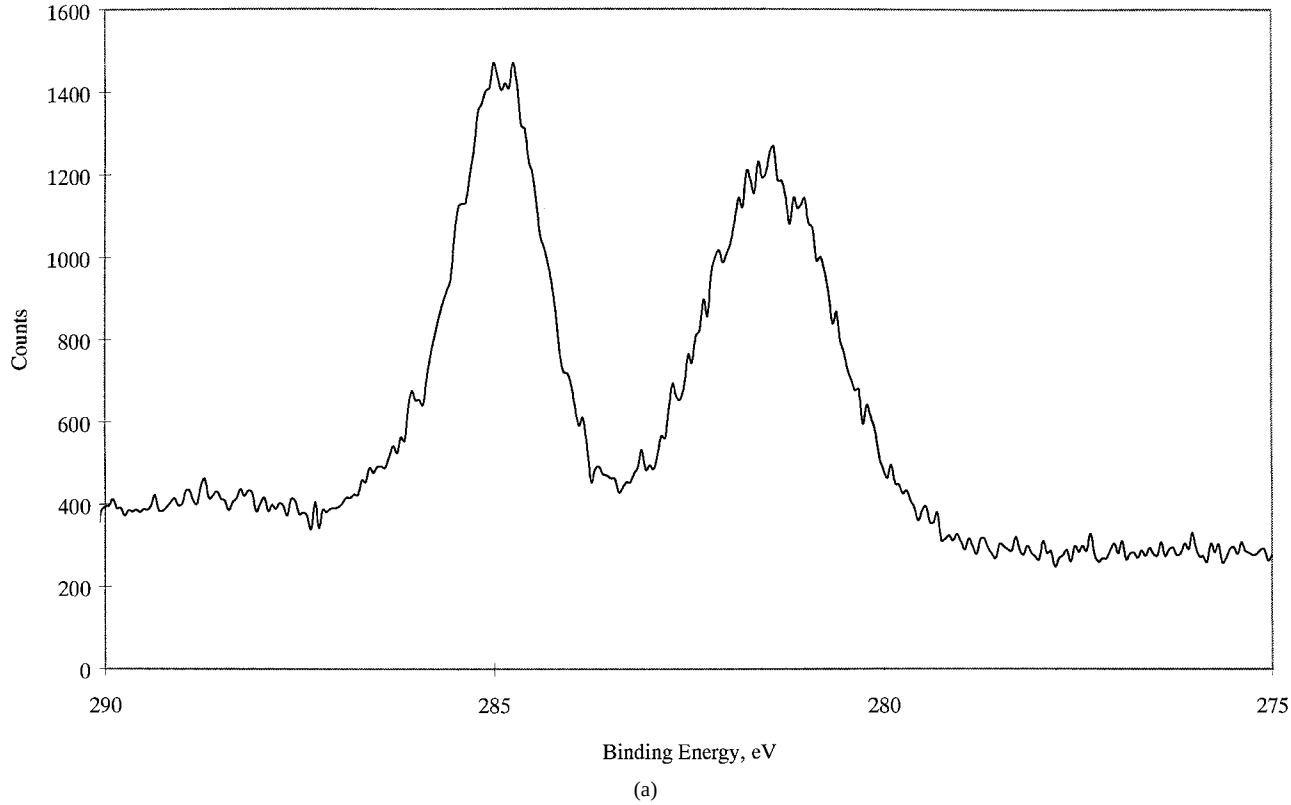

(a)

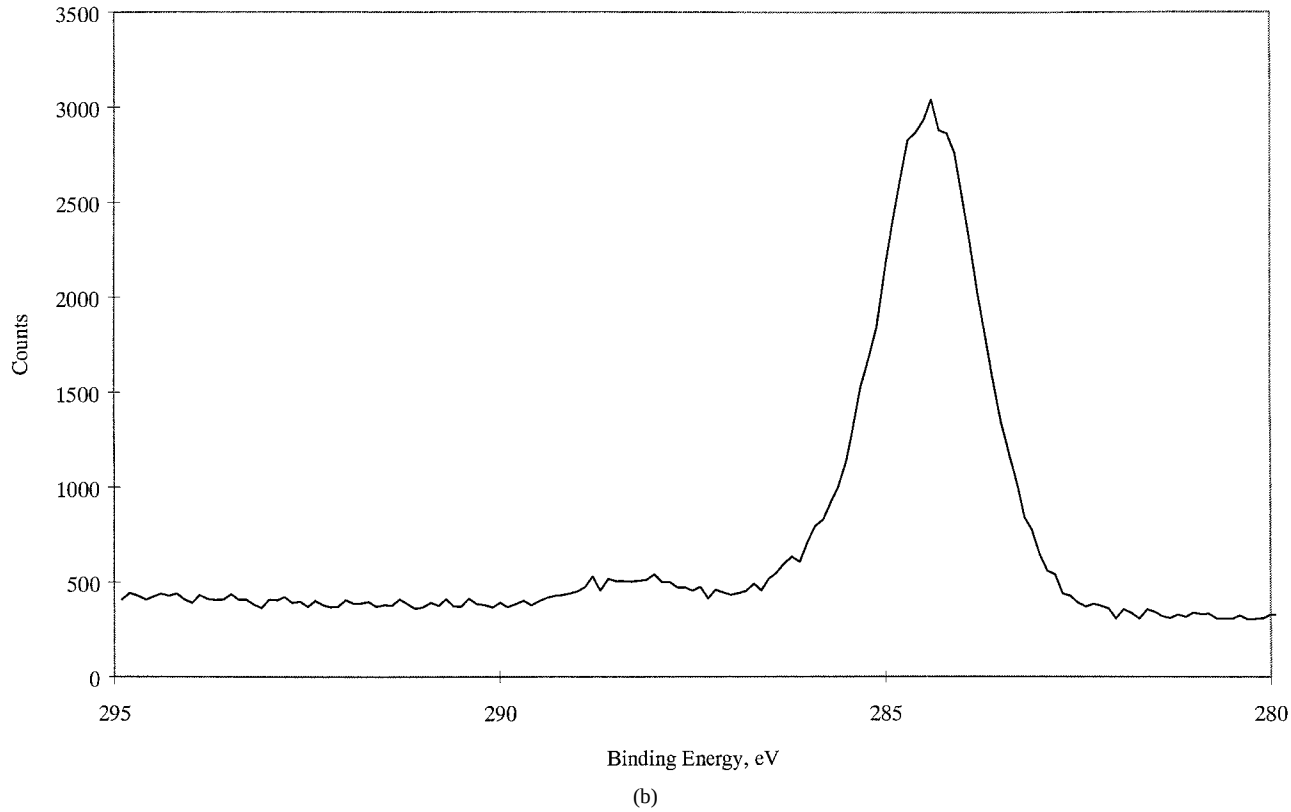

(b)

Figure 6 C 1s spectra of HMDSO plasma polymer on titanium which had failed to sustain dropwise condensation after ~ 5 000 h exposure to steam. (a) Scienta ESCA300 spectrometer (electron take-off-angle = 10°). (b) Kratos AXIS HSI spectrometer (electron take-off-angle = 90°).

signal/noise ratio of these spectra is due to the fact that a small aperture was used, as discussed in Section 3.2.

Three spectral components could be distinguished in the case of the O 1s spectra (O1, O2 and O3) with varying relative intensities at different points. The Si 2p region always displayed two peaks, Si1 and Si2. The Ti 2p doublets recorded at the four locations were identical except for the varying peak intensity (data not shown). Charge correction was accomplished using the Ti $2p_{3/2}$ peak as a reference. Taking into account the characteristics of the charge neutralization facility of the AXIS HSI system, the corrected binding energy appeared to

Figure 7 Scanning electron micrograph of titanium substrate after coating failure.

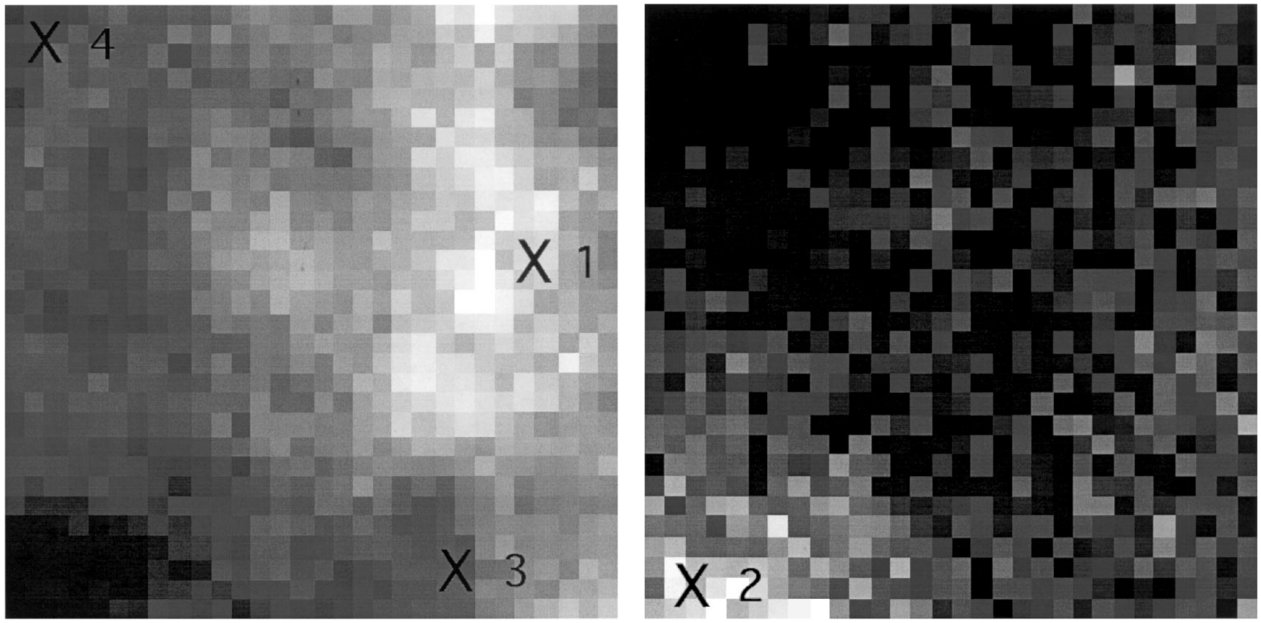

Figure 8 Elemental maps showing the distribution of (a) titanium and (b) silicon on the surface of a HMDSO plasma polymer coating on titanium which has failed to sustain dropwise condensation after ~5 000 h exposure to steam. Maps acquired in the Kratos AXIS HSI spectrometer. Points at which a spectroscopic analysis was performed are marked (see Fig. 9).

be close to the reference value for TiO_2 (458.8 eV) [34]. Using this value to correct all spectra yielded a mean position of 530.1 eV for the lower binding energy component O1 of the O 1s spectrum, consistent with TiO_2 [34]. The ratio of the corresponding fractions (O1:Ti) was found to be just over 2:1, again consistent with TiO_2. For the remainder of this discussion it should be noted that distinctly different phases or surface layers might charge differently during analysis; this probably explains some of the deviations between the measured binding energy values and the reference values.

The two Si 2p components were observed at 102.5 eV, assigned to silicon in a siloxane environment and 104.5 eV. The latter value is very high and can only be due to either silica-type materials or possibly silanols. The two higher binding energy components of the O 1s spectrum appeared at ~ 532.2 eV (O2) and 534.8 eV (O3). Based on the binding energy and the fact that the ratios of corresponding fractions (O2:Si1 and O3:Si2) did not vary appreciably from one point on the sample to the next, we assign O2 to the siloxane-type coating and O3 to either silica-type materials or silanols [34]. Fig. 10 displays the results of quantifying the detected species using non-linear least-squares curve fitting. As expected from the qualitative information provided by the maps shown in Fig. 8, point 1 showed substantial amounts of TiO_2 and a correspondingly low level of species related to the plasma-HMDSO-coating. The situation was reversed in the case of point 2 where the coating clearly dominated the overall surface composition of the sample. The results from points 3 and 4 proved to be particularly interesting in that the fractions of Si2 and O3, tentatively assigned to silica/silanols, were substantially higher compared to the other two points. This would suggest that an interfacial layer existed between the TiO_2 and the plasma HMDSO coating, which

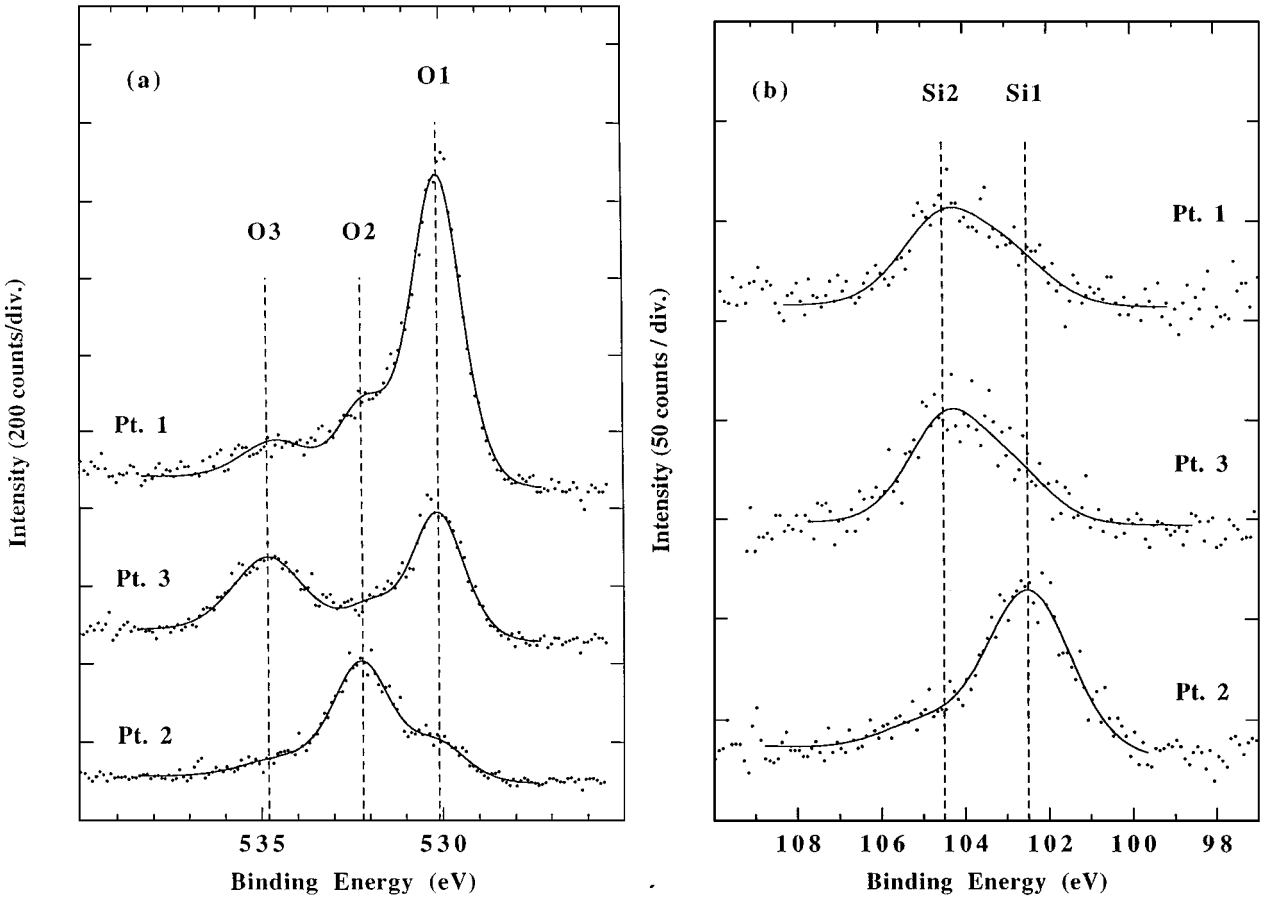

Figure 9 Photoelectron spectra of HMDSO plasma polymer on titanium which has failed to sustain dropwise condensation after ~ 5000 h exposure to steam. Kratos AXIS HSI spectrometer (electron take-off-angle = 90°). Spectra were acquired at points 1, 2, 3 (and 4) on the sample as marked on the titanium map in Fig. 8. (a) Oxygen 1s region. (b) Silicon 2p region.

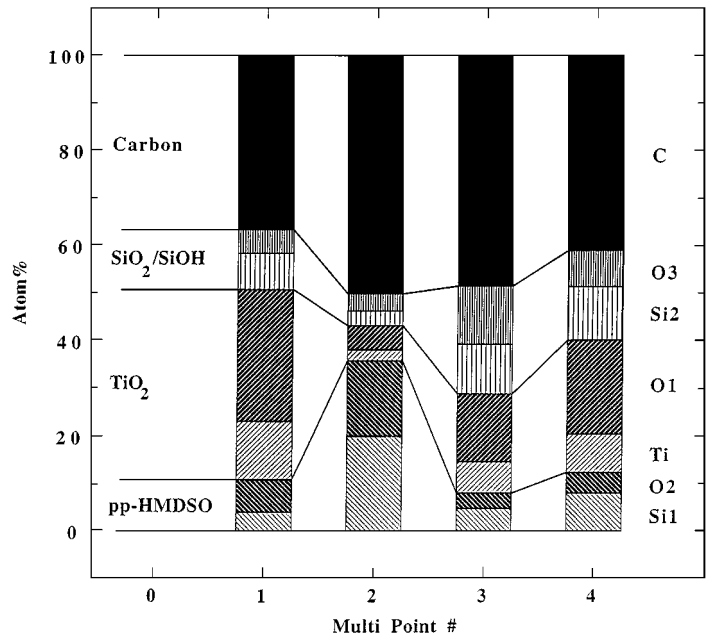

Figure 10 Quantification of detected species at four analysis points on XPS maps by non-linear least-squares curve fitting.

could only be detected in areas where the coating had just been removed.

Therefore, our data indicate the following structure prior to steam testing. The titanium substrate was covered by a layer of TiO_2 of at least 5–10 nm thick (taking into account the sampling depth of XPS which did not detect any titanium metal). An ultrathin film of SiO_x had formed on the substrate followed by the actual pp-HMDSO coating. We speculate that during the initial phase of HMDSO plasma deposition, the deposited material is of an inorganic nature (silica), whereas the remainder of the coating has the typical organosilicon

structure as observed by XPS (see Section 4.1). (This is consistent with reports by Wróbel *et al*. [20, 35] that plasma polymerized HMDSO films have a layer adjacent to the substrate that is denser than the outer, weaker cross-linked, surface layer.) This interstitial layer might well account for the comparatively good adhesion of the plasma polymer to the TiO_2 substrate because it would bond well to both TiO_2 and the siloxane-based plasma-deposited material. We note that the ratio of O3:Si2 was always less than 2:1 which is inconsistent with pure SiO_2. In our experience, however, this is a common phenomenon: once SiO_2 is exposed to (humid) air, water adsorbs on the surface, leading to the formation of silanols. These are stable for extended periods of time even under ultrahigh vacuum. Considering that the coated samples had been exposed to steam for > 5000 h our finding is not surprising.

4.3. XPS of steam-exposed tubes

The titanium tube surfaces which underwent steam testing at elevated steam velocities (10, 30 and 50 m s^{-1}) revealed a marked decrease in durability with increasing steam velocity. This was a more rapid failure mechanism compared with that observed in the long-term testing of flat specimens in steam at less than 2 m s^{-1}.

XPS was used to analyse the outer surfaces of three tube sections at different stages of steam testing: before exposure to steam, after 6 h exposure to steam at 10 m s^{-1} and after 8 h exposure to steam at 50 m s^{-1}. As expected, the coated tube before exposure consisted of carbon, oxygen and silicon. However, a very small amount of titanium was also detected (1.4%) possibly due to the film being very thin or the presence of pinholes. The coated tube which was exposed to steam at 10 m s^{-1} continued to condense dropwise for the 6 h duration of the test. XPS analysis on a section of this tube revealed carbon, oxygen and silicon and a small amount of sodium. The sodium has almost certainly come from boiler water additives but it is interesting to note that no titanium peak was present on this sample. The absence of the titanium peak may be due to a greater film thickness than with the previous sample and thus even after exposure to steam, the film was not thinned sufficiently to expose the substrate. The final analysis was on a tube which had been exposed to high-velocity steam (50 m s^{-1}) for $\sim$ 8 h until no dropwise condensation was apparent on the tube surface. XPS analysis of this specimen showed a large amount of carbon with oxygen, titanium and a small sodium contribution, as before. Results are tabulated in Table III. None of the coating was visibly left intact and this complete removal was confirmed by the absence of any Si 2p signal in the XPS spectra.

TABLE III Elemental atomic concentrations for plasma-polymerized HMDSO on titanium tube, including XPS sensitivity factors, but neglecting any hydrogen content

Sample	Steam test pass/fail	Concentration (at %)				
		C	O	Si	Ti	Na
1252	Untested	54.5	23.2	20.9	1.4	0
1244	Pass	67.7	17.3	13.9	0	1.0
1242	Fail	71.2	22.0	0	4.9	1.8

5. Discussion

Long-term steam exposure of titanium coated with the HMDSO plasma polymer showed it to be the best long-term promoter of dropwise condensation in this study. An earlier section of this work has attempted to establish the best deposition conditions for long-term durability of this material. Although some specimens did fail to sustain their hydrophobic characteristics either partially or over their entire surface at various stages of testing, the titanium substrates performed far more reliably than either stainless steel or copper-nickel HMDSO plasma-coated samples.

Two reasons for the good performance of the coated titanium substrates are proposed.

1. It is known that titanium has a very stable oxide [36] which passivates the surface, providing a high resistance to further oxidation.

2. A strong chemical bond between the titanium oxide layer and the plasma polymer coating via an interfacial layer of a silicon oxide, formed during the initial stages of plasma deposition, resulted in improved adhesion between coating and substrate.

However, the presence of Al_2O_3 contamination in the titanium substrates has led to questions over the pretreatment but it is unclear why no such contamination was found on the other substrate materials. One explanation would be the initial roughness/ease of polishing. In passing it should be mentioned that images obtained using an atomic force microscope (AFM) concur with the suggestion that the Al_2O_3 pits form localized failure sites, where attack by water vapour and subsequent expansion causes the plasma polymer to swell and delaminate. The coating itself seems to resist extensive chemical changes (oxidation, hydrolysis) as indicated by the absence of significant amounts of CO_2R/CO_2H functionality in the XPS spectra.

The complete coating removal obviously highlights a problem with coating durability at increased steam velocities. Although the steam condition was approximately saturated, de-superheating from an initial steam temperature of around 15 °C was required. This was done using a spray de-superheating technique and inevitably water droplets are propelled along with the flow. It is accepted that droplet impingement on tubes in high-velocity steam causes severe erosion problems [37] and perhaps the geometry of how the steam enters the condenser unit needs to be examined if the application of a hydrophobic plasma polymer layer on to utility turbine condenser tubes is to become commercially feasible.

6. Conclusion

For HMDSO plasma polymer films deposited on to metal substrates, no obvious correlation between initial air/water contact angles nor chemical composition by XPS and dropwise condensation lifetime, was apparent.

It was shown that the chemical composition of the plasma polymer films was not critically dependent on the deposition conditions and only small variations in chemical composition were observed.

Long-term low-velocity steam condensation tests of flat specimens, plasma-coated with HMDSO, revealed a strong substrate dependence: films deposited on to titanium performed well, many with lifetimes in excess of 12 000 h. For those flat specimens which failed, the proposed failure mechanism is permeation of water through the plasma polymer film, which results in chemical attack at the interface and hydrolysis of Al_2O_3 contamination spots, which leads to pinhole corrosion. The coating is forced to lift and the result is localized film removal and failure to sustain DWC. Sample cleaning and pre-treatment needs to be closely examined and perhaps a more rigorous solvent clean and/or ion bombardment should be considered to remove Al_2O_3 contamination.

In the case of coated tube sections tested in steam at elevated velocities, the failure mechanism is thought to involve rapid erosion and subsequent removal of the plasma polymer film. This is thought to be caused by impingement of small water droplets in the steam flow.

Acknowledgements

The authors thank EPSRC for continuing financial support. Work at the RUSTI facility (Daresbury Laboratories) was funded by an EPSRC allocation (RG113 and RG131). Mark Bonnar acknowledges the Sir James Caird Trust for supporting a study visit to CSIRO.

References

1. H. K. YASUDA (ed.), *J. Appl. Polym. Sci. Appl. Polym. Symp.* **42** (1988).
2. *Idem, ibid.* **46** (1990).
3. HERMAN VON BOENIG, "Fundamentals of Plasma Chemistry and Technology" (Technomic Publishing, Lancaster, PA, 1988).
4. R. D'AGOSTINO (ed.) "Plasma Deposition, Treatment and Etching of Polymers" (Academic Press, New York, 1990).
5. M. R. WERTHEIMER, J. E. KLEMBERG-SAPIEHA and H. P. SCHREIBER, *Thin Solid Films* **115** (1984) 109.
6. A. M. WROBEL and M. R. WERTHEIMER, in "Plasma Deposition, Treatment and Etching of Polymers," edited by R. d'Agostino (Academic Press, San Diego, 1990).
7. N. INAGAKI, "Plasma Surface Modification and Plasma Polymerisation" (Technomic Publishing, Lancaster, PA, 1996).
8. The BOC inc., "Process for plasma enhanced CVD of anti-fog and anti-scratch coatings onto various substrates," Australian pat. AU 9515026 9601 (1995).
9. H. GRUNWALD, M. JUNG, R. KUKLA, R. ADAM and S. KUNKEL, in "Proceedings of a Workshop on Industrial Applications of Plasma Chemistry," Vol. A, August 1995, edited by J. Wendt and H. Heberlein.
10. S. EUFINGER, W. J. VAN OOIJ and K. D .CONNERS, *Surf. Interface Anal.* **24** (1996) 841.
11. S. F. DURRANT, R. P. MOTA and M. A. BICA DE MORAES, *Vacuum* **47** (1996) 187.
12. J. A. THEIL, J. G. BRACE and R. W. KNOLL, *J. Vac. Sci. Technol. A* **12** (1994) 1365.
13. K. KASHIWAGI, Y. YOSHIDA and Y. MURAYAMA, *Japn. J. Appl. Phys* **30** (1991) 1803.
14. SHIDE CAI, JIANGLIN FANG and XUEHAI YU, *J. Appl. Polym. Sci.* **44** (1992) 135.
15. C. BOURREAU, Y. CATHERINE and P. GARCIA, *Plasma Chem. Plasma Process.* **10** (1990) 247.
16. F. JANSEN and S. KROMMENHOEK, *Thin Solid Films* **252** (1994) 32.
17. H.-U. POLL, J. MEICHSNER, M. ARZT, M. FRIEDRICH, R. ROCHOTZKI and E. KREYSSIG, *Surf. Coatings Technol.* **59** (1993) 365.
18. R. ROCHOTZKI, M. ARZT, F. BLASCHTA, E. KREYSSIG and H.-U. POLL, *Thin Solid Films* **234** (1993) 463.
19. R. P. MOTA, D. GALVAO, S. F. DURRANT, M. A. BICA DE MORAES, S. DE OLIVEIRA DANTAS and M. CANTAO, *ibid.* **270** (1995) 109.
20. A. M. WRÓBEL, M. R. WERTHEIMER, J. DIB and H. P. SCHREIBER, *J. Macromol. Sci. Chem.* **A14** (1980) 321.
21. E. RADEVA, D. TSANKOV, K. BOBEV and L. SPASSOV, *J. Appl. Polym. Sci.* **50** (1993) 165.
22. I. H. COOPES and H. J. GRIESSER, *ibid.* **37** (1989) 3413.
23. M. R. ALEXANDER, R. D. SHORT, F. R. JONES, M. STOLLENWERK, J. ZABOLD and W. MICHAELI, *J. Mater. Sci.* **31** (1996) 1879.
24. C. RAU and W. KULISCH, *Thin Solid Films* **249** (1994) 28.
25. M. P. BONNAR, B. M. BURNSIDE, A. LITTLE, R. L. REUBEN and J. I. B. WILSON, *Adv. Mater. CVD* **3** (1997) 201.
26. A. QAYYUM, J. I .B. WILSON, F. IBRAHIM and S. K. AL SABBAGH, "Compositional study of glow discharge hydrogenated amorphous silicon-carbon alloys from silane-propane mixtures," E-MRS Meeting, Strasbourg, June 1987, **xvii** (Les Editions de Physique, Paris, 1987) p. 463.
27. B. M. BURNSIDE and Q. ZHAO, in Eurotherm Seminar No. 47, "Heat Transfer in condensation," edited by R. Vidil and C. H. Marvillet (Elsevier, Lausanne, 1996).
28. H. A. HADI and R. L. REUBEN, D. T. I, National Power, Multi Arc Collaborative Project report No. 5, N.P. EPS/0108; D. T. I WM 93/115 (1993).
29. G. BEAMSON, D. BRIGGS, S. F. DAVIES, I. W. FLETCHER, D. T. CLARK, HOWARD, U. GELIUS, B. WANNBERG and P. BALZER, *Surf. Interface Anal.* **15** (1990) 541.
30. G. BEAMSON and D. BRIGG, "High resolution XPS of organic polymers: The Scienta ESCA300 database" (Wiley, New York, 1992).
31. B. J. TIELSCH and J. E. FULGHUM, *Surf. Interface Anal.* **24** (1996) 28.
32. E. SACHER, J. KLEMBERG-SAPIEHA, H. P. SCHREIBER, N. S. WERTHEIMER and N. S. MCINTYRE, in "Proceedings of the Chemically Modified Surfaces Symposium," Midland, Michigan, Vol. 1 (1985).
33. H. J. GRIESSER, in "Polymers in Information Storage Technology," edited by K. L. Mittal (Plenum, New York, 1989) p. 351.
34. C. D. WAGNER, W. M. RIGGS, L. E. DAVIS, J. F. MOULDER and G. E. MUILENBERG, "Handbook of X-Ray Photoelectron Spectroscopy" (Perkin-Elmer Corporation, Physical Electronics Division, Minnesota, 1979).
35. A. M. WRÓBEL and G. CZEREMUSZKIN, *Thin Solid Films* **216** (1992) 203.
36. "Titanium Offshore," January 1996 (The Titanium Information Group, c/o David Peacock, Timet, UK Ltd.) p. 16.
37. European Federation of Corrosion Publications, "Illustrated Case Histories of Marine Corrosion," Number 5 (1990) p. 126.

Received 27 August 1997
and accepted 22 April 1998